Sensitive detection of MCF-7 human breast cancer cells by using a novel DNA-labeled sandwich electrochemical biosensor

Yuhan Yang, Yongyao Fu, Huilan Su, Li Mao, Mei Chen

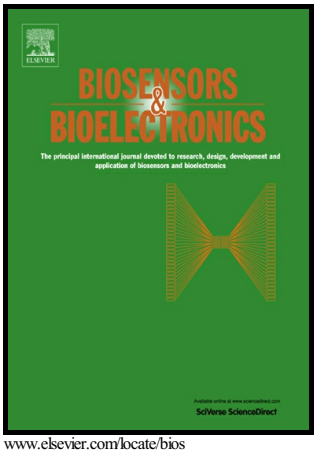

www.elsevier.com/locate/bios

PII: S0956-5663(18)30752-8
DOI: https://doi.org/10.1016/j.bios.2018.09.062
Reference: BIOS10802

To appear in: *Biosensors and Bioelectronic*

Received date: 14 June 2018
Revised date: 15 September 2018
Accepted date: 17 September 2018

Cite this article as: Yuhan Yang, Yongyao Fu, Huilan Su, Li Mao and Mei Chen, Sensitive detection of MCF-7 human breast cancer cells by using a novel DNA-labeled sandwich electrochemical biosensor, *Biosensors and Bioelectronic,* https://doi.org/10.1016/j.bios.2018.09.062

Sensitive detection of MCF-7 human breast cancer cells by using a novel DNA-labeled sandwich electrochemical biosensor

Yuhan Yang [a], Yongyao Fu [b], Huilan Su [c], Li Mao[c], Mei Chen [a]*

[a] School of biology science and technology, Chengdu medical college, Chengdu, Sichuan 610500, PR China

[b] School of advanced agriculture and bioengineering, Yangtze normal university, Fuling District, chongqing, 408100, china

[C] School of public health, Chengdu medical college, Chengdu 610500, PR China

* Corresponding author: Mei Chen. Tel.: +862862739583; fax: +862862739582.

E-mail address: 396762073@qq.com. (M. Chen).

Abstract

The simple, rapid, sensitive, and specific detection of cancer cells plays a pivotal role in the diagnosis and prognosis of cancer. We developed a novel DNA-labeled sandwich electrochemical biosensor based on a glassy carbon electrode modified with 3D graphene and a hybrid of Au nanocages (Au NCs)/amino-functionalized multiwalled carbon nanotubes (MWCNT-NH_2) for label-free and selective detection of MCF-7 breast cancer cells via differential pulse voltammetry. The layer-by-layer assembly and cell-detection performance of the Au NCs/MWCNTs-NH_2-based biosensor were investigated using scanning electron microscopy and electrochemical methods including cyclic voltammetry and electrochemical impedance spectroscopy. Owing to the advantages of DNA-labeled antibodies and a nanomaterial-based signal amplification strategy, the fabricated cytosensor exhibited high specificity and sensitivity when detecting MCF-7 cells in the range of 1.0×10^2 to 1.0×10^6 cells mL^{-1} with a low detection limit of 80 cells mL^{-1} (3σ/slope). Furthermore, the biosensor exhibited high selectivity when detecting MCF-7 cells and showed considerable potential for practical applications. The proposed DNA-labeled sandwich electrochemical biosensor provides a stable, sensitive approach to detecting cancer cells and is promising in terms of potential applications to cancer diagnosis.

Keywords: Sandwich electrochemical biosensor; DNA-labeled probe; Au nanocage; MWCNT-NH_2; MCF-7 cells

1. Introduction

In 2016, more than 18 million people were reported to be suffering from cancer

and approximately 9.6 million deaths were caused by cancer (Cronin et al. 2018; Shi et al. 2017). In particular, breast cancer was the second-most common cause of death in women, with most deaths resulting from neoplasm metastasis (Min and Shou 2016). The identification and sensitive detection of cancer cells is of great importance owing to the urgent demand for rapid and highly effective methods of early diagnosis of cancer (Williams et al. 2016). However, as only very low concentrations of circulating tumor cells are present in the peripheral blood, the detection of cancer cells with high specificity and sensitivity remains challenging (Liu et al. 2016). Currently, several technologies have been employed for cancer diagnosis, including the polymerase chain reaction (Tan et al. 2015), immunohistochemistry (Chaudhary et al. 2015), and flow cytometry (Les et al. 2016). However, some of these methods are relatively complicated, time-consuming, and expensive, while others have unsatisfactory sensitivity and specificity (Emran et al. 2018; Manzano et al. 2018). Therefore, the development of a rapid, selective, and economic approach to detecting cancer cells is highly required.

Recent years have witnessed great developments in the field of electrochemical biosensors for rapid, selective, and sensitive cancer-cell detection at low cost (Dong et al. 2017; Uliana et al. 2018; Wang et al. 2017). Li et al. (2011) constructed an aptamer-based electrochemical immunosensor for detecting early apoptotic cells by using aptamer-modified quantum dots on the surface of a gold electrode and polyethylene glycol as a membrane material. Xu et al. (2015) used three-dimensional (3D) multiwalled carbon nanotubes (MWCNTs) bound to molecules of a specific ligand 2-(*p*-aminophenyl)-1,3,2-dithiarsenolane to construct a sensor that detects tumor cells in which vicinal dithiol-containing proteins are overexpressed. However, to the best of our knowledge, no electrochemical biosensors have been reported for the capture and sensitive detection of cancer cells based on DNA-modified antibody probes. The ssDNA-modified antibody probes avoid the process of abzyme labeling, are highly stable, and offer high capture efficiency (Liu et al. 2015). Therefore, in this study, we developed a novel electrochemical immunosensor based on DNA-modified antibodies for the detection of MCF-7 breast cancer cells.

The use of 3D nanostructured electrodes is highly desirable for improvements in the performance of electrochemical biosensors (Guo et al. 2015; Song et al. 2015). In nanomaterial-based systems, Au-based nanoparticles (NPs) are highly efficient catalysts that facilitate a large number of reactions (Tian et al. 2018), including oxygen reduction and alkene hydrogenation (Zhang et al. 2017), and have been utilized in immunoassays (Torati et al. 2016). Recently, considerable effort has been devoted to the fabrication of hollow metallic spheres, as they can provide larger specific surface areas in comparison with their solid counterparts, and because they can achieve better catalytic effects (Huang et al. 2015; Khan et al. 2012). Au nanocages (NCs) are innovative materials in the field of biosensing with hollow interiors and porous walls (Liu et al. 2015; Robinson et al. 2015). Wang et al. (2014a) demonstrated that well-aligned MWCNTs are important for improving the sensitivity of electrochemical detection. MWCNTs are promising materials for electrochemical biosensors because of their high electronic conductivity, chemical stability, large

surface area, and extremely high mechanical strength (Jin et al. 2017). Moreover, owing to the hydrophilicity of primary amines, MWCNTs-NH_2 have high dispersity in water and are promising supports for large-scale loading of other nanomaterials or biomolecules. Therefore, we used Au NCs-MWCNTs-NH_2 as a nanostructured surface to construct an inexpensive and sensitive electrochemical biosensor.

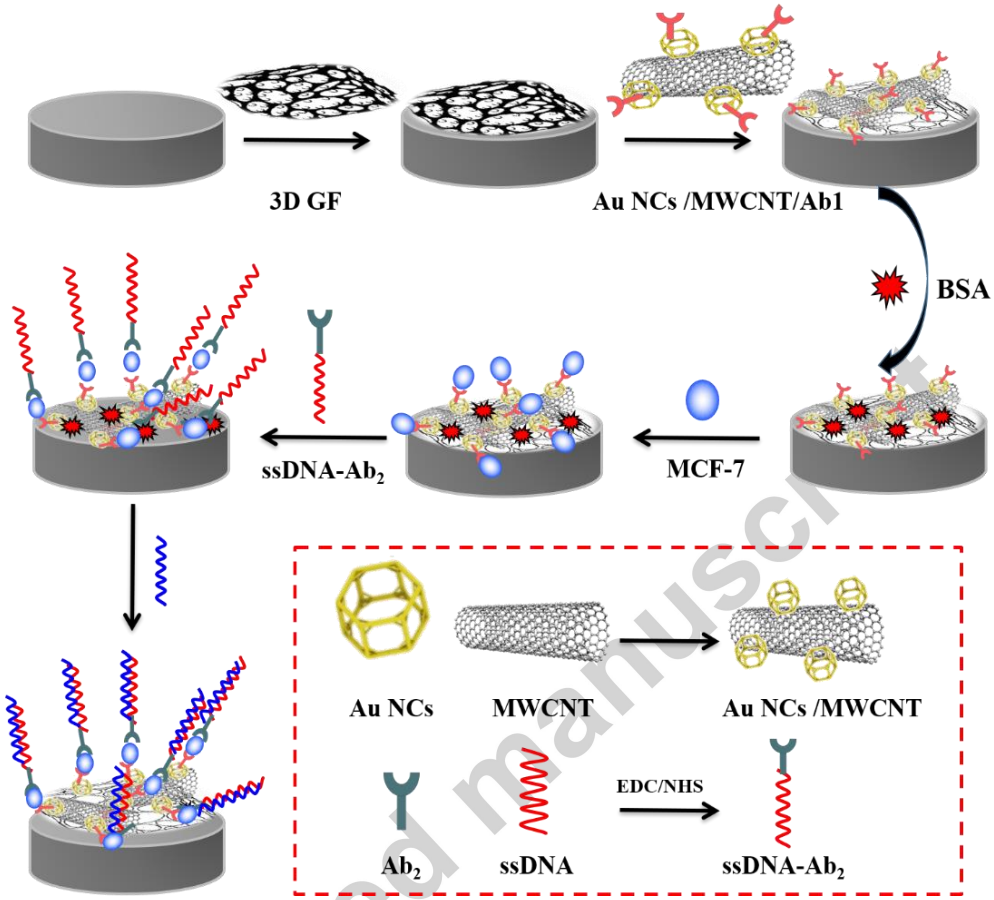

Figure 1. Schematic representation of the formation of the immunosensor with the DNA marker antibody.

In this study, we developed a novel sandwich-type biosensor for the electrochemical determination of MCF-7 human breast cancer cells. The proposed biosensor combines the advantages of DNA-labeled antibodies and a nanomaterial-based signal amplification strategy. First, we synthesized 3D graphene (GF) as an ideal electrode substrate. We then synthesized Au NCs-functionalized MWCNTs as a substrate for the adsorption of breast-cancer estrogen receptor (ER) antibodies (Ab_1). ER is highly expressed on the surface of breast cancer cells. Hence, the specific recognition of ER was used to adsorb and immobilize MCF-7 breast cancer cells on the sensor (Hajra et al. 2002; Zghair et al. 2016). The 5' end of a single-stranded DNA (ssDNA) was linked to a breast-cancer ER antibody (Ab_2) by using the coupling agent 1-ethyl-3-(3-dimethylaminopropyl) carbodiimide (EDC) + N-hydroxysuccinimide (NHS). Thus, an ssDNA-Ab_2 biological probe comprising an ssDNA marker antibody was synthesized. Owing to the specificity of the identification of ER by Ab_2, the ssDNA-Ab_2 probe was fixed to the modified

electrode. This approach avoids the process of abzyme labeling, offers strong capture efficiency and significantly amplifies the detection signal by using a sandwich-type biomimetic interface with high biocompatibility and stability.

2. Experiment

2.1. Apparatus and Materials

Electrochemical measurements were performed using a CHI 600D electrochemical workstation with a conventional three-electrode system. A platinum wire counter electrode was used as an auxiliary electrode, and an Ag/AgCl electrode was used as a reference electrode. Samples were morphologically characterized using an FEI Nova 400 field-emission scanning electron microscope and a Zeiss Libra 200 transmission electron microscope (TEM). Methylene blue, Tris-HCl, dicyclohexylcarbodiimide (DCC), and ethylenediamine (EDA) were purchased from Sigma-Aldrich (St. Louis, MO, USA). Other reagents were purchased from Chongqing Chuandong Chemical Co., Ltd. All chemicals were of analytical grade, and deionized (DI) water was obtained using a Milli-Q water purification system (Bedford, MA, USA).

The probe DNA and target oligonucleotides were synthesized and purified using Sangon Biological Engineering Technology Co., Ltd (Shanghai, China). Stock solutions of all oligonucleotides were prepared with 0.01 M phosphate-buffered saline (PBS, pH 7.4) and stored at 4 °C. The respective base sequences were as follows:
Probe DNA: 5′-GAAGGGAGGAATGGTGTCAGGGGCG-3′.
Complementary target DNA: 5′-CGCCCCTGACACCATTCCTCCCTTC-3′.
One-base mismatched target DNA: 5′-CGCCCCTGACACCATTCCTCCCTTC-3′.
Three-base mismatched target DNA: 5′-CGCGCCTGACTCCATTCCTCCCATC-3′.
Non-complementary target DNA: 5′-TTGTCCAGGTAGGAGGCCAGGCGGT-3′.

2.2. Synthesis of MWCNTs-NH_2

Carboxyl-modified MWCNTs (MWCNTs-COOH) were synthesized from MWCNTs according to the method by Li et al. (2015). MWCNTs were treated with a 3:1 mixture of concentrated H_2SO_4 and HNO_3 (98% and 70%, respectively) under ultrasonication for 4 h at 40 °C. Then, the MWCNTs were rinsed with triply distilled water until the pH level was nearly neutral. Subsequently, the precipitate that formed was dried in a vacuum drying oven at 40 °C for 12 h. MWCNTs-NH_2 were prepared by the condensation reaction of –COOH and –NH_2 groups; the reaction was conducted by the addition of 0.4 g DCC to a solution of 20 mg MWCNTs-COOH in 2.5 mL EDA. The reaction mixture was stirred for 96 h at 120 °C. After centrifugation, the resulting MWCNTs-NH_2 were obtained after washing, and dried in vacuum at 35 °C.

2.3. Synthesis of Au NCs/MWCNTs-NH_2

In brief, polyvinylpyrrolidone (PVP, 1 mg/mL) was added to 5 mL DI water to form a homogeneous solution, and then 500-mL Ag nanocubes (3 nM) were added to this solution, which was then boiled for 10 min. Subsequently, $HAuCl_4$ (0.5 mM) was added to the flask at a rate of 45 mL/h. The solution was refluxed for another 30 min until the color of the reaction mixture was stable. After cooling it to room temperature, the sample was centrifuged and washed with a saturated solution of NaCl to remove AgCl, and then washed three times with water to remove PVP and NaCl.

The prepared MWCNTs-NH_2 were dispersed in the solution of synthesized Au NCs by stirring for 12 h and centrifuged under mild conditions (2000 rpm) for 5 min. The procedure of changing the supernatant illustrated whether the solution of Au NCs was slightly excessive. Au NCs/MWCNTs-NH_2 were obtained through centrifugation and dried in vacuum at 35 °C.

2.4. Preparation of Au NCs/MWCNTs-NH_2/Ab_1 labels and ssDNA-Ab_2 probes

A solution of Au NCs/MWCNTs-NH_2 (2 mg/mL, 1 mL) was added to a dispersion of Ab_1 (10 mg/mL, 1 mL) and stirred for 12 h at 4 °C. After centrifugation, the resulting Au NCs/MWCNTs-NH_2/Ab_1 labels were dispersed in 1 mL PBS at a pH of 7.4 and stored at 4 °C.

By using ssDNA-tagged molecules of Ab_2, a dispersion of Ab_2 (5 μg/mL) was added to a 10-mM solution of PBS containing 2.12×10^{-6} M ssDNA and a 0.1-M solution of EDC/NHS. After mixing and incubating them for 1 h at room temperature, the solutions of the resulting ssDNA-Ab_2 probes were stored at 4 °C until they were used.

2.5. Cytotoxicity assay

MCF-7 breast cancer cells were seeded in a 96-well plate at a density of 5×10^3 cells per well, and cultured in an atmosphere of 5% CO_2 at 37 °C for 24 h. Then, Au NCs/MWCNTs-NH_2 were added to the medium, and the cells were incubated in 5% CO_2 at 37 °C for 12 h. The concentrations of Au NCs/MWCNTs-NH_2 were 0, 3.8, 7.6, 15.2, 30.4, 60.8, and 121.6 mg/mL. The cytotoxicity was assessed using a 3-(4,5-dimethylthiazol-2-yl)-2,5-diphenyltetrazolium bromide (MTT) assay.

2.6. Fabrication of the immunosensor

A glassy carbon electrode (GCE) was wet-polished to give a mirror-like surface. Next, 6-μL of a 1.5-mg/mL solution of 3D GF was dropped onto the pretreated electrode (see Fig. 1). After drying, 3 -μL EDC/NHS was added to the electrode, and 10-μL Au NCs/MWCNTs-NH_2/Ab_1 (2 mg/mL) was immediately dropped onto the electrode. After incubation at 4 °C and washing, the electrode was incubated in a 1 wt% solution of bovine serum albumin (BSA) for 30 min to eliminate nonspecific binding. The obtained immunosensor was stored at 4 °C until it was used.

The electrode immunosensor, prepared earlier, was immersed in solutions of

MCF-7 breast cancer cells at different concentrations for 1 h at 37 °C and then washed with ultrapure water. Subsequently, solutions of ssDNA-Ab_2 were dropped. The electrode was again incubated in a 1 wt% solution of BSA for 30 min to eliminate nonspecific binding. Then, solutions of the prepared Au NCs/MWCNTs-NH_2/Ab_2 were dropped onto the modified electrode surface. The prepared biosensor was immersed in 0.01 M PBS containing target DNA at 50 °C for 50 min, and the surface of the ssDNA-Ab_2 probe molecule was hybridized with complementary DNA. The hybridized electrode was incubated in a 20 μM MB solution for 20 min and then washed with 0.1 wt% SDS in PBS (pH 7.0). Finally, the electrochemical measurements were performed. Square-wave voltammetry responses (SWVs) were obtained within a potential range of −1.0 and −0.3 V at a scan rate of 0.1 V/s. Electrochemical impedance spectra (EIS) were analyzed in a frequency range of 10^6–0.1 Hz at an AC amplitude of 5 mV. SWV and EIS were analyzed in a solution of 0.1-M KCl containing 1.0-mM $[Fe(CN)_6]^{3-/4-}$. Finally, the electrochemical response was determined through differential pulse voltammetry (DPV) in a 0.1-M PBS (pH 7.0) with respect to pulse amplitude and width of 50 mV and 0.05 s, respectively.

3. Results and discussion

3.1. Characterization of Au NCs and Au NCs/MWCNTs-NH_2

As shown in Fig. 2A, the color of the Au NPs is orange–purple, whereas the Au NCs appear blue. The UV–Vis spectrum of a solution of the Au NCs is shown in Fig. 2B. It can be observed that the UV spectrum of the Au NCs displays a strong absorption peak centered at 800 nm; this is the typical characteristic absorption peak and is consistent with that observed in the reported literature (Wang et al. 2014b). Scanning electron microscopy (SEM) images demonstrated that the Au NCs were well dispersed and exhibited high uniformity (Figs. 2C and 2D). More details were revealed through TEM images (Figs. 2E and 2F). The size of the Au NCs, which had hollow structures, was approximately 30–50 nm. The N_2 adsorption-desorption isotherms of the Au NCs are given in Figure S1. The specific surface area of the Au NPs and Au NCs calculated using the multipoint Brunauer–Emmett–Teller (BET) method is 58.9 m^2 g^{-1} and 143.6 m^2 g^{-1} with the adsorption data at the relative pressure (P/P_0), respectively. This indicates that the fabrication of the Au NCs materials could increase their specific surface area owing to their hollow spherical shape.

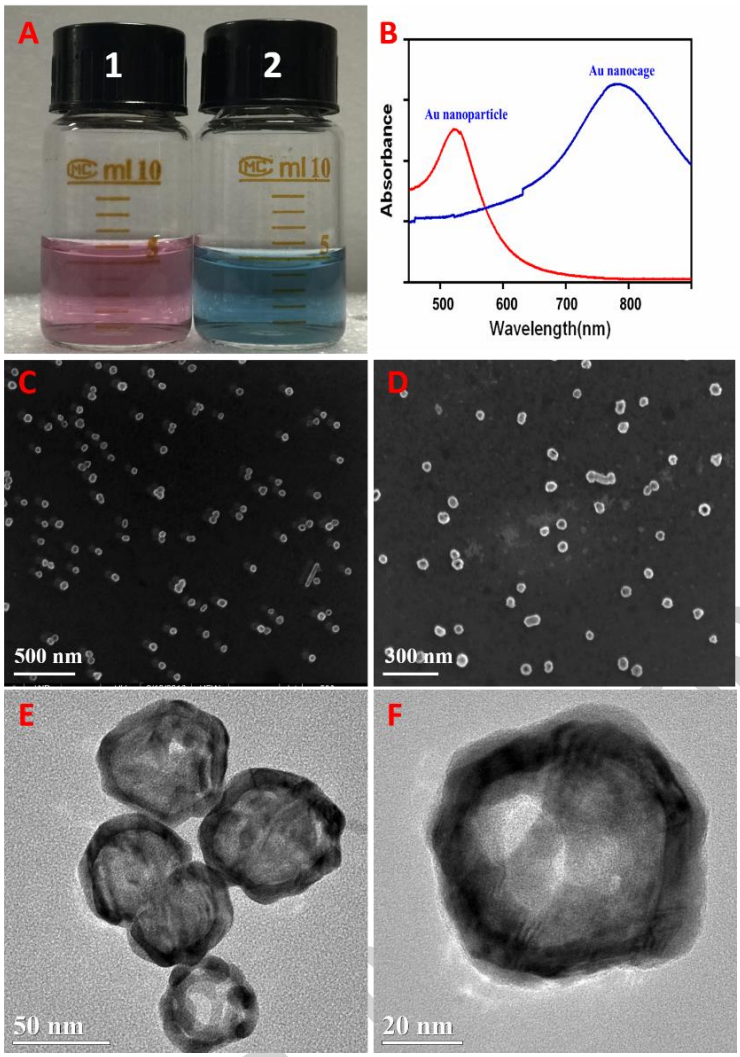

Figure 2. (A) Photograph of (1) Au NPs and (2) Au NCs. (B) UV absorption spectra of Au NPs and Au NCs. (C, D) SEM images of Au NCs. (E) TEM and (F) high-resolution TEM images of Au NCs.

After the MWCNTs-NH_2 were mixed with the Au NCs, and large numbers of Au NCs were successfully linked to the surfaces of the MWCNTs-NH_2 (Figs. 3A and 3B), providing direct evidence that the Au NCs were decorated on the MWCNTs-NH_2. The corresponding lattice fringes can be observed in a high-resolution TEM image (HRTEM; Figs. 3C and 3D). Fig. 3D shows an interplanar spacing of approximately 0.24 nm, which is in good agreement with the d-spacing of the (111) lattice plane of Au NCs. Moreover, there were numerous pores on the surface of each Au NCs/MWCNT-NH_2; this might be of great significance for catalytic applications, as the pores will increase the specific surface area and facilitate electron transfer.

3.2. Cytotoxicity assay

The precise cytotoxicity of a probe must be determined before applying it to living cells. In this study, cell cytotoxicity studies of the Au NCs/MWCNTs were

performed using an MTT assay, in which MCF-7 breast cancer cells were incubated with different concentrations of Au NCs/MWCNTs for 24 h. As shown in Fig. 4A, the MCF-7 cells in the control group were well formed, with long fusiform or ovoid shapes, and round cells were also visible. The cells in the experimental group (Fig. 4B) were basically similar to those in the control group; the majority of the cells were well shaped and their walls were growing, and discrete particles were present in the cytoplasm. As shown in Fig. 4C, the cell viability decreased slightly with an increase in the Au NCs/MWCNTs concentration. At a concentration of 45 μg/mL, 84.5% of the MCF-7 breast cancer cells survived with respect to the control group after incubation for 24 h; this suggests that the Au NCs/MWCNTs had low cytotoxicity. The low toxicity and high biocompatibility of the prepared Au NCs/MWCNTs make them promising for biological applications.

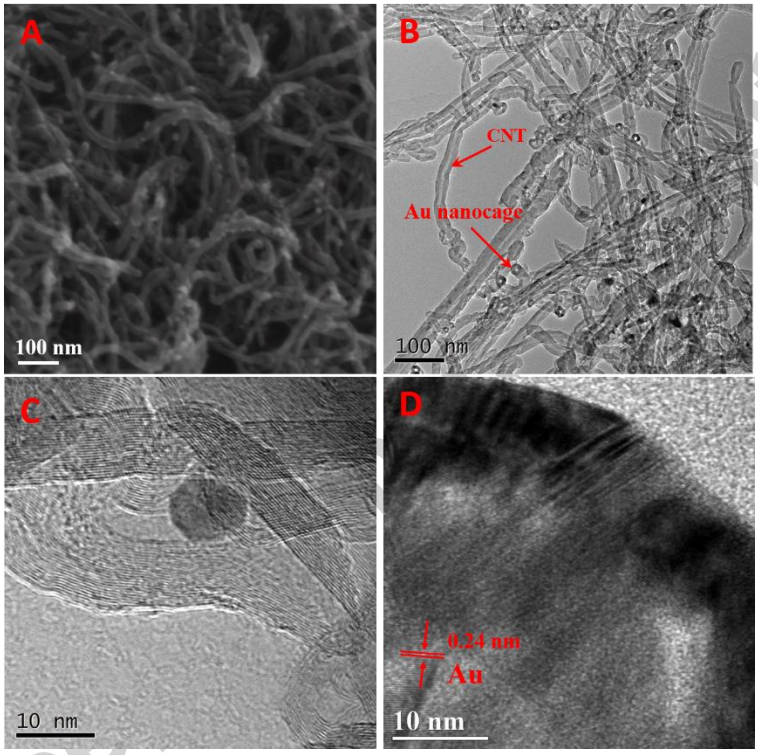

Figure 3. (A, B) SEM images of Au NCs/MWCNTs-NH_2. (C) TEM and (D) high-resolution TEM images of Au NCs/MWCNTs-NH_2.

3.3 Comparison of different signal amplification strategies

To demonstrate the significance of Au NCs/MWCNTs-NH_2 as the catalytic label of Ab_1 for signal amplification in the proposed biosensor, different signaling labels, including Au NPs/GCE, Au NCs/GCE, Au NPs+MWCNTs/GCE, and Au NCs+MWCNTs/GCE, were used to design immunosensors (Fig. 5A). Compared with other similar sensors, the immunosensor using Au NCs/MWCNTs-NH_2 as the label exhibited a much higher electrochemical response. This result may be attributed to the following two factors. First, the use of MWCNTs-NH_2 as a support is attractive because MWCNTs-NH_2 have useful properties, such as high electronic conductivity,

chemical stability, high dispersity in water, and the ability to facilitate electron transfer to amplify the current signal and improve the stability of the biosensor. Second, hollow Au NCs, as a novel material, provide larger specific surface areas and more exposed active sites, and exhibit excellent electrocatalytic activity.

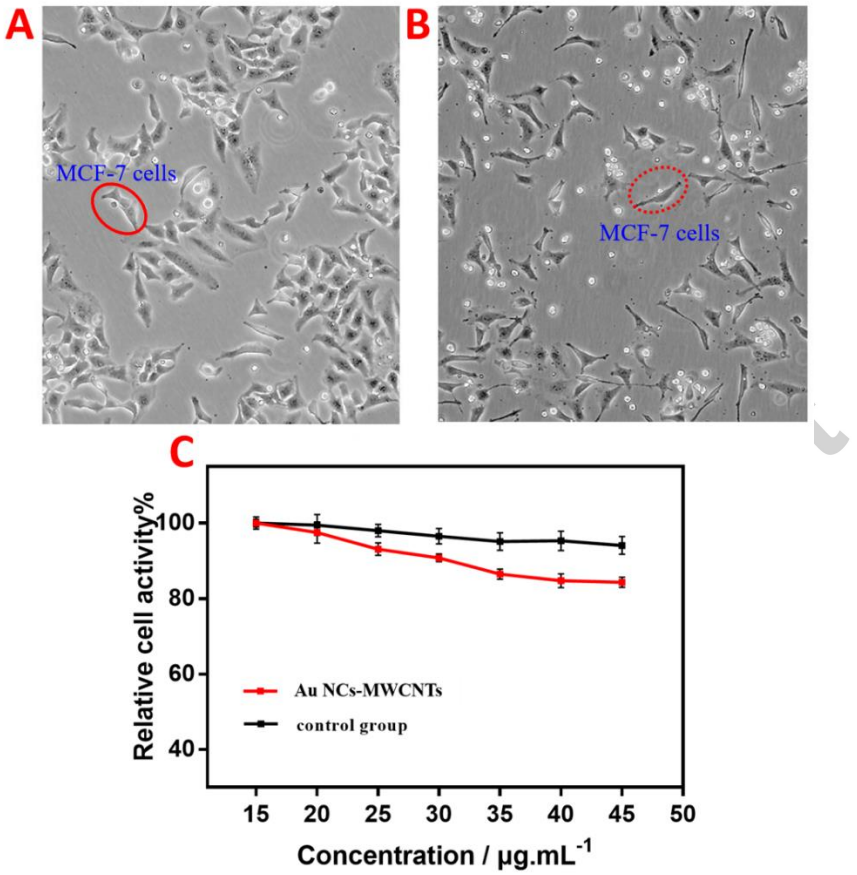

Figure 4. Morphological images of cells: (A) control group and (B) experimental group. (C) Cell viabilities of human MCF-7 cells incubated with Au NCs/MWCNTs-NH_2 with different concentrations for 24 h.

3.4 Electrochemical behavior of the modified electrode

EIS is one of the most powerful tools for studying the stepwise modification processes of the proposed electrode (Wei et al. 2018). Fig. 5B shows the Nyquist plots of the impedance spectra recorded at different electrodes in a solution of 0.1 M KCl containing 1.0 mM $[Fe(CN)_6]^{3-/4-}$. The diameter of the semicircle in the impedance spectrum equals the electron transfer resistance (R_{et}).

Undoubtedly, the R_{et} value of the 3D GF-modified electrode (curve b) is much lower than that of the bare electrode (curve a). When Au NCs/MWCNTs/Ab_1 were dropped onto the 3D GF/GCE, as seen in the Nyquist plot, the R_{et} value increased significantly (curve c). Although the Au NCs/MWCNTs had high conductivity, the antibody biomacromolecules greatly impeded electron transfer. Subsequently, the R_{et} value increased further after the MCF-7 cells were successively adsorbed onto the electrode surface (curve d); this is consistent with the fact that the hydrophobic layer

of MCF-7 cells and BSA insulate the conductive support and hinder interfacial electron transfer. Next, when ssDNA+Ab_2 were immobilized on the modified electrode, the value of R_{et} also increased (curve e), indicating that ssDNA+Ab_2 were successfully immobilized on the surface of MCF-7 cells. When the probe was hybridized with the target DNA to form a double-stranded DNA (dsDNA), the value of R_{et} increased owing to the large amount of negatively charged DNA linked to the electrode surface (curve f). As a result, the immunosensor was successfully constructed.

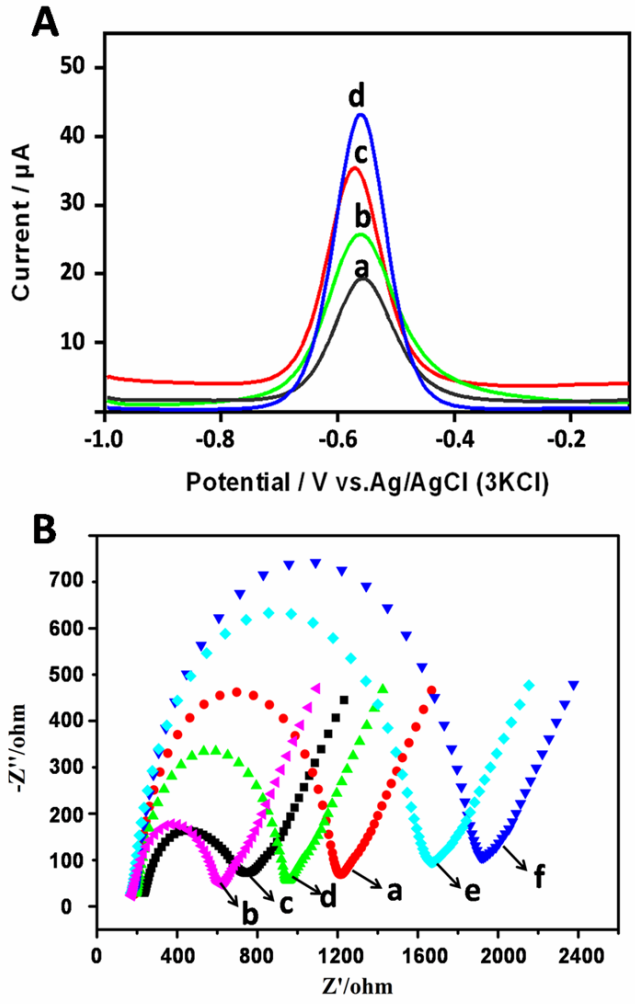

Figure 5. (A) SWV response of different modified electrodes: (a) Au NPs/GCE, (b) Au NCs/GCE, (c) Au NPs+MWCNTs /GCE, and (d) Au NCs+MWCNTs /GCE. (B) EIS characteristics of the modified electrodes in a solution of 0.1-M KCl containing 1.0-mM $[Fe(CN)_6]^{3-/4-}$: (a) bare GCE, (b) 3D GF/GCE, (c) 3D GF/Au NCs+MWCNTs/Ab_1/GCE, (d) MCF-7/3D GF/Au NCs+MWCNTs /Ab_1/GCE, (e) ssDNA-Ab_2/MCF-7/3D GF/Au NCs+MWCNTs/Ab_1/GCE, and (f) dsDNA-Ab_2/MCF-7/3DGF/Au NCs+MWCNTs/Ab_1/GCE.

3.5 Optimization of experimental conditions

The pH value of the electrolyte solution can also influence the activity of the biomolecules. To obtain an optimal electrochemical signal, the response signal in PBS

was tested systematically with different pH values (from 5.5 to 8.5), and the experimental results (Fig. S3A) revealed that the maximum amperometric response occurred at a pH of 7.4. Thus, PBS with a pH of 7.4 was appropriate for subsequent tests. The effect of the immunochemical incubation time is an important parameter affecting the response of animmunosensor. The immunosensors were incubated with 20-ng/mL antibody for different durations. As shown in Fig. S3B, the response signals increased and then remained at a maximum value after 60 min. Therefore, an incubation time of 60 min was selected for later experiments.

3.6 Quantitative detection of MCF-7 cells

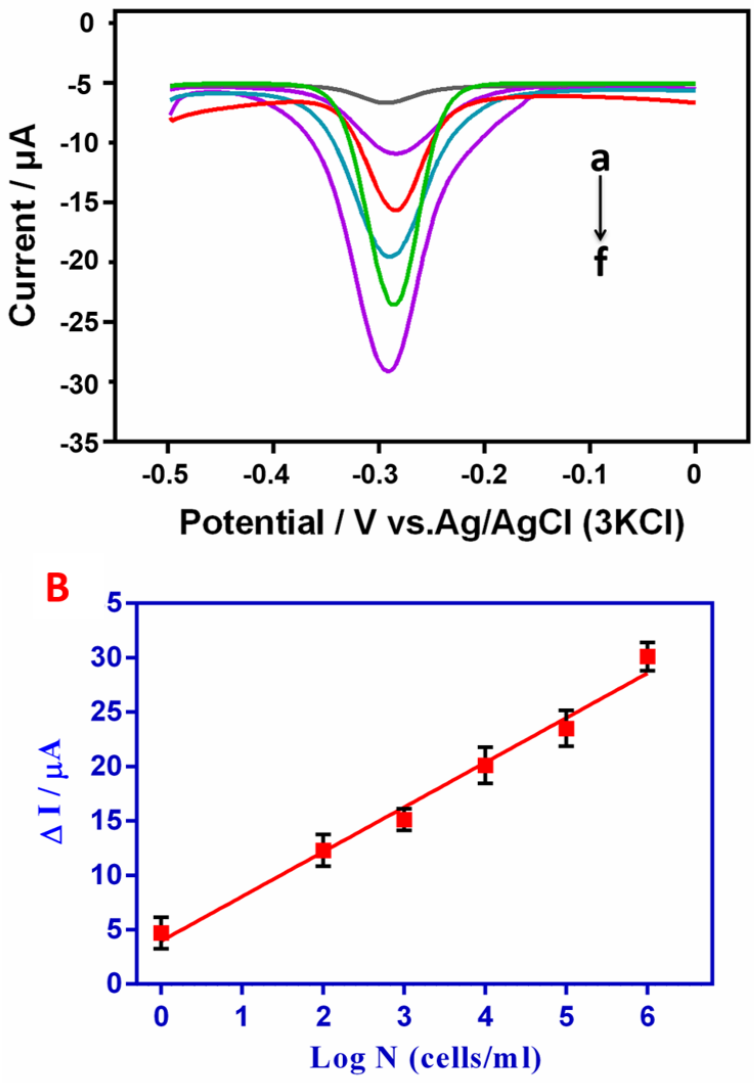

Figure 6. (A) DPV response of MCF-7 cells after hybridization with target DNA. The number of MCF-7 cells (cells mL^{-1}) was as follows: 0, 1.0×10^2, 1.0×10^3, 1.0×10^4, 1.0×10^5, and 1.0×10^6 (curves a-f, respectively). (B) Plot of peak current vs. log of concentration (cells mL^{-1}).

Under optimized conditions, the sandwich-type immunosensors were used to detect MCF-7 cells. To assess the sensitivity of our assay, suspensions of MCF-7 cells

with different concentrations were prepared by diluting a stock suspension of the cells. As indicated in Fig. 6A, the DPV peak currents in the electrochemical assay increased with an increase in the concentration of MCF-7 cells, and a linear relationship was exhibited between the increase DPV peak current (ΔI) and concentration C of the MCF-7 cells in the range from 0 to 1.0×10^6 cells mL^{-1} (Fig. 6B). The regression equation was ΔI (μA) = 4.104 log C +3.958 (correlation coefficient R =0.9868), with a detection limit (LOD) as low as 80 cells mL^{-1}. Moreover, a wide detection range was obtained based on the calculation of 3σ /slope. The sensitivity of the present immunosensor based on Au NCs/MWCNTs-NH_2/Ab_2 is superior to that of many reported biosensors for MCF-7 detection, as listed in Table S1.

The excellent performance was ascribed to the signal-amplification strategy of the proposed sandwich-type electrochemical immunosensor. The novelty and advantages of the immunosensor are as follows. First, the Au NCs/MWCNTs-NH_2 has a large surface area and excellent conductivity; these play an essential role not only in binding large numbers of Ab_1 molecules and MCF-7 cells but also in assisting the electron transfer process. Second, the use of hollow Au NCs, which provide more exposed active sites, is an innovative step in the field of biosensing. Moreover, owing to their high biocompatibility, hollow Au NCs can provide an appropriate biological environment. Third, the ssDNA-Ab_2 probe is highly stable and offers high capture efficiency and strong specific binding.

3.7 Selectivity, reproducibility, and stability of the immunosensor

To assess the selectivity of the electrochemical biosensor, it was incubated in a solution of carcinoembryonic antigen containing 10^5 cells mL^{-1} of different interfering substances: HeLa cells (human cervical carcinoma cells), NEC cells (human pancreatic cancer adjacent tissue cells), CEC cells (human pancreatic cancer cells), and MCF-7 cells. As illustrated in Fig.S4, the HeLa, NEC 293, and CEC cells show a light current change after incubation in the sensing system but the MCF-7 cells show a well-defined current change. These current changes depend on the cell type and selectivity of DNA-labeled probe. This result demonstrates that the proposed biosensor is highly selective when detecting MCF-7 cells and has considerable potential for clinical applications.

To assess the reproducibility of the biosensor, five electrodes were prepared for the detection of MCF-7 cells. The relative standard deviation (RSD) of measurements using the five electrodes was less than 4.6%. In addition, the stability of the immunosensor was also studied (Fig.S5). More than 90.6% of the initial response (n = 5, RSD = 3.9 %) remained constant after storage at 4 °C for 14 days. Consequently, the reproducibility and stability of the proposed immunosensor are acceptable.

4. Conclusions

We designed a new sandwich biosensor (ssDNA-Ab_2/MCF-7/Ab_1) based on 3D GF, Au NCs/MWCNTs-NH_2, for the detection of MCF-7 human breast cancer cells.

Owing to the advantages of DNA-labeled antibodies and a nanomaterial-based signal-amplification strategy, this biosensor showed a wider linear range and a lower detection limit. This approach avoids the process of abzyme labeling, offers high capture efficiency, and significantly amplifies the detection signal through the use of a sandwich-type biomimetic interface with high biocompatibility and stability. Therefore, by using simple and effective 3D nanoscale components assembled on a sensing surface and DNA-labeled antibodies, this electrochemical cytosensing approach provides a feasible and sensitive method for detecting cancer cells with considerable potential for clinical applications to the early diagnosis of cancer.

Acknowledgments

The authors would like to acknowledge the financial support from "the Scientific Research Fund of Sichuan Provincial Education Department (No. 18ZA0137)", "Research project of Sichuan Provincial Health and Planning Biology Committee (No.18PJ113)", "National Natural Science Foundation of Chengdu Medical College (N.O. 17Z122)" and "the National Natural Science Foundation of China (N.O. 81401757 and N.O.81601859)".

References

Chaudhary, L.N., Jawa, Z., Szabo, A., Visotcky, A., Chitambar, C.R., 2015. Inverse relationship between ER plus /PR-breast cancer and OncotypeDx scores and concordance between IHC and RT-PCR. Cancer Res 75(9).

Cronin, K.A., Lake, A.J., Scott, S., Sherman, R.L., Noone, A.M., Howlader, N., Henley, S.J., Anderson, R.N., Firth, A.U., Ma, J., Kohler, B.A., Jemal, A., 2018. Annual Report to the Nation on the Status of Cancer, part I: National cancer statistics. Cancer 124(13), 2785-2800.

Dong, H., Zhang, L., Liu, W., Tian, Y., 2017. Label-Free Electrochemical Biosensor for Monitoring of Chloride Ion in an Animal Model of Alzhemier's Disease. Acs Chem Neurosci 8(2), 339-346.

Emran, M.Y., Mekawy, M., Akhtar, N., Shenashen, M.A., El-Sewify, I.M., Faheem, A., El-Safty, S.A., 2018. Broccoli-shaped biosensor hierarchy for electrochemical screening of noradrenaline in living cells. Biosens Bioelectron 100, 122-131.

Guo, J., Zhang, T., Hu, C., Fu, L., 2015. A three-dimensional nitrogen-doped graphene structure: a highly efficient carrier of enzymes for biosensors. Nanoscale 7(4), 1290-1295.

Hajra, K.M., Chen, D.Y., Fearon, E.R., 2002. The SLUG zinc-finger protein represses E-cadherin in breast cancer. Cancer Res 62(6), 1613-1618.

Hao, C., Ding, L., Zhang, X., Ju, H., 2007. Biocompatible conductive architecture of carbon nanofiber-doped chitosan prepared with controllable electrodeposition for cytosensing. Anal Chem 79(12), 4442-4447.

Huang, Y.H., Chen, J.H., Ling, L.J., Su, Z.B., Sun, X., Hu, S.R., Weng, W., Huang, Y., Wu, W.B., He, Y.S., 2015. Simultaneous electrochemical detection of catechol and hydroquinone based on gold nanoparticles@carbon nanocages modified electrode. Analyst 140(23), 7939-7947.

Hui, W., Tian, W., Yan-Xia, Y., Zhang, Y.-X., Pei-Hui, Y., Huai-Hong, C., Ji-Ye, C., 2012. Construction of an electrochemical cytosensor based on polyaniline nanofiber/gold nanoparticle interface and application to detection of cancer cells. Chinese J Anal Chem 40(2), 184-190.

Jin, M., Zhang, X., Zhen, Q., He, Y., Chen, X., Lyu, W., Han, R., Ding, M., 2017. An electrochemical

sensor for indole in plasma based on MWCNTs-chitosan modified screen-printed carbon electrode. Biosens Bioelectron 98, 392-397.

Khan, S.A., Kanchanapally, R., Fan, Z., Beqa, L., Singh, A.K., Senapati, D., Ray, P.C., 2012. A gold nanocage–CNT hybrid for targeted imaging and photothermal destruction of cancer cells. Chem Commun 48(53), 6711-6713.

Les, T., Markiewicz, T., Osowski, S., Kozlowski, W., Jesiotr, M., 2016. Fusion of FISH image analysis methods of HER2 status determination in breast cancer. Expert Syst Appl 61, 78-85.

Li, J., Xu, M., Huang, H., Zhou, J., Abdel-Halimb, E.S., Zhang, J.R., Zhu, J.J., 2011. Aptamer-quantum dots conjugates-based ultrasensitive competitive electrochemical cytosensor for the detection of tumor cell. Talanta 85(4), 2113-2120.

Li, N., Wang, Y., Cao, W., Zhang, Y., Yan, T., Du, B., Wei, Q., 2015. An ultrasensitive electrochemical immunosensor for CEA using MWCNT-NH2 supported PdPt nanocages as labels for signal amplification. J Mater Chem B 3(9), 2006-2011.

Liu, F., Ge, S., Su, M., Song, X., Yan, M., Yu, J., 2015. Electrochemiluminescence device for in-situ and accurate determination of CA153 at the MCF-7 cell surface based on graphene quantum dots loaded surface villous Au nanocage. Biosens Bioelectron 71, 286-293.

Liu, J., Chen, X., Ward, T., Pegram, M., Shen, K., 2016. Combined niclosamide with cisplatin inhibits epithelial-mesenchymal transition and tumor growth in cisplatin-resistant triple-negative breast cancer. Tumour Biol.

Manzano, M., Viezzi, S., Mazerat, S., Marks, R.S., Vidic, J., 2018. Rapid and label-free electrochemical DNA biosensor for detecting hepatitis A virus. Biosens Bioelectron 100, 89-95.

Min, L., Shou, C., 2016. In Situ Hybridization of Breast Cancer Markers. Methods in molecular biology 1406, 53-59.

Robinson, R., Gerlach, W., Ghandehari, H., 2015. Comparative effect of gold nanorods and nanocages for prostate tumor hyperthermia. J Control Release 220(Pt A), 245-252.

Shi, J., Kantoff, P.W., Wooster, R., Farokhzad, O.C., 2017. Cancer nanomedicine: progress, challenges and opportunities. Nature reviews. Cancer 17(1), 20-37.

Song, H., Yang, L., Tang, Y., Yan, D., Liu, C., Luo, S., 2015. Three-Dimensional Nitrogen-Doped Reduced Graphene Oxide-Carbon Nanotubes Architecture Supporting Ultrafine Palladium Nanoparticles for Highly Efficient Methanol Electrooxidation. Chemistry 21(46), 16631-16638.

Tan, V., Baehner, F., Yoshizawa, C., Anderson, J., Bailey, H., Tsiatis, A., Sing, A.P., Shak, S., 2015. Quantitative RT-PCR gene expression in the special histologic subtypes of invasive breast cancer. Breast 24, S38-S39.

Tian, L., Qian, K., Qi, J., Liu, Q., Yao, C., Song, W., Wang, Y., 2018. Gold nanoparticles superlattices assembly for electrochemical biosensor detection of microRNA-21. Biosens Bioelectron 99, 564-570.

Torati, S.R., Reddy, V., Yoon, S.S., Kim, C., 2016. Electrochemical biosensor for Mycobacterium tuberculosis DNA detection based on gold nanotubes array electrode platform. Biosens Bioelectron 78, 483-488.

Uliana, C.V., Peverari, C.R., Afonso, A.S., Cominetti, M.R., Faria, R.C., 2018. Fully disposable microfluidic electrochemical device for detection of estrogen receptor alpha breast cancer biomarker. Biosens Bioelectron 99, 156-162.

Wang, K., He, M.Q., Zhai, F.H., He, R.H., Yu, Y.L., 2017. A novel electrochemical biosensor based on polyadenine modified aptamer for label-free and ultrasensitive detection of human breast cancer cells. Talanta 166, 87-92.

Wang, X., Wu, M., Li, H., Wang, Q.J., He, P.N., Fang, Y.Z., 2014a. Simultaneous electrochemical determination of hydroquinone and catechol based on three-dimensional graphene/MWCNTs/BMIMPF6 nanocomposite modified electrode. Sensor Actuat B-Chem 192, 452-458.

Wang, Z., Chen, Z., Liu, Z., Shi, P., Dong, K., Ju, E., Ren, J., Qu, X., 2014b. A multi-stimuli responsive gold nanocage-hyaluronic platform for targeted photothermal and chemotherapy. Biomaterials 35(36), 9678-9688.

Wei, Y.P., Liu, X.P., Mao, C.J., Niu, H.L., Song, J.M., 2018. Highly sensitive electrochemical biosensor for streptavidin detection based on CdSe quantum dots. Biosens Bioelectron 103, 99-103.

Williams, C.B., Yeh, E.S., Soloff, A.C., 2016. Tumor-associated macrophages: unwitting accomplices in breast cancer malignancy. NPJ Breast Cancer 2.

Xu, Y., Wu, H., Huang, C., Hao, C., Wu, B., Miao, C., Chen, S., Jia, N., 2015. Sensitive detection of tumor cells by a new cytosensor with 3D-MWCNTs array based on vicinal-dithiol-containing proteins (VDPs). Biosens Bioelectron 66, 321-326.

Zghair, A.N., Sinha, D.K., Kassim, A., Alfaham, M., Sharma, A.K., 2016. Differential Gene Expression of BRCA1,ERBB2 and TP53 biomarkers between Human Breast Tissue and Peripheral Blood Samples of Breast Cancer. Anticancer Agents Med Chem 16(4), 519-525.

Zhang, Y., Zhang, C., Ma, R., Du, X., Dong, W., Chen, Y., 2017. An ultra-sensitive Au nanoparticles functionalized DNA biosensor for electrochemical sensing of mercury ions. Mater Sci Eng C Mater Biol Appl 75, 175-181.

Highlights

- This work constructs a novel DNA-labeled antibodies sandwich electrochemical biosensor.
- 3D graphene@Au NCs/MWCNTs-NH_2 providing an excellent platform for nanomaterial-based signal amplification strategy.
- This electrochemical cytosensing approach avoids the process of abzyme labeling,
  offers high capture efficiency and strong specific binding.
- The electrochemical biosensor offered high sensitivity and selectivity toward human MCF-7 breast cancer cells.